

1 **A comparison of performance of several artificial intelligence**
2 **methods for forecasting monthly discharge time series**

3
4 **Wen-Chuan Wang**

5 Ph.D., Institute of hydropower system & Hydroinformatics, Dalian University of Technology,
6 Dalian, 116024, P.R. China

7 Faculty of Water conservancy Engineering, North China Institute of Water Conservancy and
8 Hydroelectric Power, Zhengzhou 450011, P.R.China

9
10 **Kwok-Wing Chau**

11 Associate Professor, Department of Civil and Structural Engineering, Hong Kong Polytechnic
12 University, Hung Hom, Kowloon, Hong Kong (Corresponding author): E-mail address:
13 cekwchau@polyu.edu.hk Tel.: (+852) 2766 6014

14
15 **Chun-Tian Cheng**

16 Professor, Institute of hydropower system & Hydroinformatics, Dalian University of Technology,
17 Dalian, 116024, P.R. China

18
19 **Lin Qiu**

20 Professor, Institute of environmental & municipal engineering, North China Institute of Water
21 Conservancy and Hydroelectric power, ZhengZhou, 450011, P.R.Ch

22
23 **Abstract.** Developing a hydrological forecasting model based on past records is crucial to
24 effective hydropower reservoir management and scheduling. Traditionally, time series analysis and
25 modeling is used for building mathematical models to generate hydrologic records in hydrology
26 and water resources. Artificial intelligence (AI), as a branch of computer science, is capable of
27 analyzing long-series and large-scale hydrological data. In recent years, it is one of front issues to
28 apply AI technology to the hydrological forecasting modeling. In this paper, autoregressive
29 moving-average (ARMA) models, artificial neural networks (ANNs) approaches, adaptive
30 neural-based fuzzy inference system (ANFIS) techniques, genetic programming (GP) models and
31 support vector machine (SVM) method are examined using the long-term observations of monthly
32 river flow discharges. The four quantitative standard statistical performance evaluation measures,
33 the coefficient of correlation (R), Nash-Sutcliffe efficiency coefficient (E), root mean squared
34 error (RMSE), mean absolute percentage error (MAPE), are employed to evaluate the
35 performances of various models developed. Two case study river sites are also provided to
36 illustrate their respective performances. The results indicate that the best performance can be
37 obtained by ANFIS, GP and SVM, in terms of different evaluation criteria during the training and
38 validation phases.

39
40 **Key words:** monthly discharge time series forecasting; ARMA; ANN; ANFIS; GP; SVM

42 **1. Introduction**

43 The identification of suitable models for forecasting future monthly inflows to hydropower
44 reservoirs is a significant precondition for effective reservoir management and scheduling. The
45 results, especially in long-term prediction, are useful in many water resources applications such as
46 environment protection, drought management, operation of water supply utilities, optimal
47 reservoir operation involving multiple objectives of irrigation, hydropower generation, and
48 sustainable development of water resources, etc. As such, hydrologic time series forecasting has
49 always been of particular interest in operational hydrology. It has received tremendous attention of
50 researchers in last few decades and many models for hydrologic time series forecasting have been
51 proposed to improve the hydrology forecasting.

52 These models can be broadly divided into three groups: regression based methods, time series
53 models and AI-based methods. For autoregressive moving-average models (ARMA) proposed by
54 Box and Jenkins (1970), it is assumed that the times series is stationary and follows the normal
55 distribution. ARMA is one of the most popular hydrologic times series models for reservoir design
56 and optimization. Extensive application and reviews of the several classes of such models
57 proposed for the modelling of water resources time series were reported (Chen and Rao, 2002;
58 Salas, 1993; Srikanthan and McMahon, 2001).

59 In recent years, AI technique, being capable of analysing long-series and large-scale data,
60 has become increasingly popular in hydrology and water resources among researchers and
61 practicing engineers. Since the 1990s, artificial neural networks (ANNs), based on the
62 understanding of the brain and nervous systems, was gradually used in hydrological prediction. An
63 extensive review of their use in the hydrological field is given by ASCE Task Committee on
64 Application of Artificial Neural Networks in Hydrology (ASCE, 2000a; ASCE, 2000b). The ANNs
65 have been shown to give useful results in many fields of hydrology and water resources research
66 (Campolo et al., 2003; Chau, 2006; Muttil and Chau, 2006).

67 The adaptive neural-based fuzzy inference system (ANFIS) model and its principles, first
68 developed by Jang (1993), have been applied to study many problems and also in hydrology field
69 as well. Chang & Chang (2001) studied the integration of a neural network and fuzzy arithmetic
70 for real-time streamflow forecasting and reported that ANFIS helps to ensure more efficient
71 reservoir operation than the classical models based on rule curve. Bazartseren et al. (2003) used
72 neuro-fuzzy and neural network models for short-term water level prediction. Dixon (2005)
73 examined the sensitivity of neuron-fuzzy models used to predict groundwater vulnerability in a
74 spatial context by integrating GIS and neuro-fuzzy techniques. Other researchers reported good
75 results in applying ANFIS in hydrological prediction (Cheng et al., 2005; Keskin et al., 2006;
76 Nayak et al., 2004).

77 Genetic Programming (GP), an extension of the well known field of genetic algorithms (GA)
78 belonging to the family of evolutionary computation, is an automatic programming technique for
79 evolving computer programs to solve problems (Koza, 1992). GP model was used to emulate the
80 rainfall-runoff process (Whigam and Crapper, 2001) and was evaluated in terms of root mean
81 square error and correlation coefficient (Liong et al., 2002; Whigam and Crapper, 2001). It was
82 shown to be a viable alternative to traditional rainfall runoff models. The GP approach was also
83 employed by Johari et al (2006) to predict the soil-water characteristic curve of soils. GP is
84 employed for modelling and prediction of algal blooms in Tolo Harbour, Hong Kong (Muttil and

85 Chau, 2006) and the results indicated good predictions of long-term trends in algal biomass. The
86 Darwinian theory-based GP approach was suggested for improving fortnightly flow forecast for a
87 short time-series (Sivapragasam et al., 2007).

88 The support vector machine (SVM) is based on structural risk minimization (SRM) principle
89 and is an approximation implementation of the method of SRM with a good generalisation
90 capability (Vapnik, 1998). Although SVM has been used in applications for a relatively short time,
91 this learning machine has been proven to be a robust and competent algorithm for both
92 classification and regression in many disciplines. Recently, the use of the SVM in water resources
93 engineering has attracted much attention. Dibike et al. (2001) demonstrated its use in rainfall
94 runoff modeling. Liong and Sivapragasam (2002) applied SVM to flood stage forecasting in
95 Dhaka, Bangladesh and concluded that the accuracy of SVM exceeded that of ANN in
96 one-lead-day to seven-lead-day forecasting. Yu et al.(2006) successfully explored the usefulness of
97 SVM based modelling technique for predicting of real time flood stage forecasting on Lan-Yang
98 river in Taiwan 1 to 6 hours ahead. Khan and Coulibaly (2006) demonstrated the application of
99 SVM to time series modeling in water resources engineering for lake water level prediction. The
100 SVM method has also been employed for stream flow predictions (Asefa et al., 2006; Lin et al.,
101 2006).

102 The major objectives of the study presented in this paper are to investigate several AI
103 techniques for modelling monthly discharge time series, which include ANN approaches, ANFIS
104 techniques, GP models and SVM method, and to compare their performance with other traditional
105 time series modelling techniques such as ARMA. Four quantitative standard statistical
106 performance evaluation measures, i.e., coefficient of correlation (R), Nash-Sutcliffe efficiency
107 coefficient (E), root mean squared error (RMSE), mean absolute percentage error (MAPE), are
108 employed to validate all models. Brief introduction and model development of these AI methods
109 are also described before discussing the results and making concluding remarks. The performances
110 of various models developed are demonstrated by forecasting monthly river flow discharges in
111 Manwan Hydropower and Hongjiadu Hydropower.

112 **2 Description of Selected Models**

113 Several AI techniques employed in this study include ANNs, ANFIS techniques, GP models and
114 SVM method. A brief overview of these techniques is presented here.

115 **2.1 Artificial Neural Networks (ANNs)**

116 Since early 1990s, ANNs, and in particular, feed-forward back-propagation perceptrons have been
117 used for forecasting in many areas of science and engineering (Chau and Cheng, 2002). An ANN
118 is an information processing system composed of many nonlinear and densely interconnected
119 processing elements or neurons, which is organized as layers connected via weights between
120 layers. An ANN usually consists of three layers: the input layer, where the data are introduced to
121 the network; the hidden layer or layers, where data are processed; and the output layer, where the
122 results of given input are produced. The structure of a feed-forward ANN is shown in Fig. 1.

123 A multi-layer feed-forward back-propagation network with one hidden layer has been used

124 throughout the study (Haykin, 1999). In a feed-forward back-propagation network, the weighted
125 connections feed activations only in the forward direction from an input layer to the output layer.
126 These interconnections are adjusted using an error convergence technique so that the network's
127 response best matches the desired response. The main advantage of the ANN technique over
128 traditional methods is that it does not require information about the complex nature of the
129 underlying process under consideration to be explicitly described in mathematical form.

130 **2.2 Adaptive neural-based fuzzy inference system (ANFIS)**

131 The ANFIS used in the study is a fuzzy inference model of Sugeno type, and is a
132 composition of ANNs and fuzzy logic approaches (Jang, 1993; Jang et al., 1997). The model
133 identifies a set of parameters through a hybrid learning rule combining the back-propagation
134 gradient descent and a least squares method. It can be used as a basis for constructing a set of
135 fuzzy IF-THEN rules with appropriate membership functions in order to generate the previously
136 stipulated input-output pairs (Keskin et al., 2006).

137 The Sugeno fuzzy inference system is computationally efficient and works well with linear
138 techniques, optimization and adaptive techniques. As a simple example, we assume a fuzzy
139 inference system with two inputs x and y and one output z . The first-order Sugeno fuzzy model, a
140 typical rule set with two fuzzy If-Then rules can be expressed as:

141 Rule 1: If x is A_1 and y is B_1 , then $f_1 = p_1x + q_1y + r_1$

142 Rule 2: If x is A_2 and y is B_2 , then $f_2 = p_2x + q_2y + r_2$

143 The resulting Sugeno fuzzy reasoning system is shown in Fig. 2. It illustrates the fuzzy
144 reasoning mechanism for this Sugeno model to derive an output function (f) from a given input
145 vector $[x, y]$. The corresponding equivalent ANFIS architecture is a five-layer feed forward net
146 work that uses neural net work learning algorithms coupled with fuzzy reasoning to map an input
147 space to an output space. It is shown in Fig.3. The more comprehensive presentation of ANFIS for
148 forecasting hydrological time series can be found in the literature (Cheng et al., 2005; Keskin et al.,
149 2006; Nayak et al., 2004).

150 **2.3 Genetic programming (GP)**

151 GP is a search methodology belonging to the class of 'intelligent' methods which allows the
152 solution of problems by automatically generating algorithms and expressions. These expressions
153 are codified or represented as a tree structure with its terminals (leaves) and nodes (functions). GP,
154 similar to GA, initializes a population that compounds the random members known as
155 chromosomes (individual). Afterward, fitness of each chromosome is evaluated with respect to a
156 target value. GP works with a number of solution sets, known collectively as a "population",
157 rather than a single solution at any one time; the possibility of getting trapped in a "local
158 optimum" is thus avoided. GP differs from the traditional GA in that it typically operates on parse
159 trees instead of bit strings. A parse tree is built up from a terminal set (the variables in the problem)
160 and a function set (the basic operators used to form the function). GP is provided with evaluation
161 data, a set of primitives and fitness functions. The evaluation data describe the specific problem in

162 terms of the desired inputs and outputs. They are used to generate the best computer program to
 163 describe the relationship between the input and output very well (Koza, 1992).

164 The representation of GP can be viewed as a parse tree-based structure composed of the
 165 function set and terminal set. The function set is the operators, functions or statements such as
 166 arithmetic operators ($\{+, -, *, /\}$) or conditional statements (if... then...) which are available in the
 167 GP. The terminal set contains all inputs, constants and other zero-argument in the GP tree. An
 168 example of such a parse tree can be found in Fig. 4. Once a population of the GP tree is initialized,
 169 the following procedures are similar to GAs including defining the fitness function, genetic
 170 operators such as crossover, mutation and reproduction and the termination criterion, etc. In GP,
 171 the crossover operator is used to swap the subtree from the parents to reproduce the children using
 172 mating selection policy rather than exchanging bit strings as in GAs.

173 The genetic programming introduced here is one of the simplest forms available. A more
 174 comprehensive presentation of GP can be found in the literature (Borrelli et al., 2006; Koza,
 175 1992).

176 2.4 Support vector machine (SVM)

177 SVM is the state-of-the-art neural network technology based on statistical learning (Vapnik, 1995;
 178 Vapnik, 1998). The basic idea of SVM is to use linear model to implement nonlinear class
 179 boundaries through some nonlinear mapping of the input vector into the high-dimensional feature
 180 space. The linear model constructed in the new space can represent a nonlinear decision boundary
 181 in the original space. In the new space, SVM constructs an optimal separating hyperplane. If the
 182 data is linearly separated, linear machines are trained for an optimal hyperplane that separates the
 183 data without error and into the maximum distance between the hyperplane and the closest training
 184 points. The training points that are closest to the optimal separating hyperplane are called support
 185 vectors. Fig. 5 exhibits the basic concept of SVM. There exist uncountable decision functions, i.e.
 186 hyperplanes, which can effectively separate the negative and positive data set (denoted by ‘x’ and
 187 ‘o’, respectively) that has the maximal margin. This indicates that the distance from the closest
 188 positive samples to a hyperplane and the distance from the closest negative samples to it will be
 189 maximized.

190 Given a set of training data $\{(x_i, d_i)\}_i^N$ (x_i is the input vector, d_i is the desired value and N is the
 191 total number of data patterns), the regression function of SVM is formulated as follows:

$$192 \quad y = f(x) = w_i \phi_i(x) + b \quad (1)$$

193 where $\phi_i(x)$ is the feature of inputs, and w_i and b are coefficients. The coefficients
 194 (w_i and b) are estimated by minimizing the following regularized risk function (Vapnik,
 195 1995; Vapnik, 1998):

$$196 \quad r(C) = C \frac{1}{N} \sum_{i=1}^N L_\varepsilon(d_i, y_i) + \frac{1}{2} \|\omega\|^2 \quad (2)$$

197 where

$$198 \quad L_\varepsilon(d, y) = \begin{cases} |d - y| - \varepsilon & \text{if } |d - y| \geq \varepsilon \\ 0 & \text{otherwise} \end{cases} \quad (3)$$

199 In Eq. (2), the first term is the empirical error (risk). They are measured by Eq. (3). $L_\varepsilon(d, y)$ is
 200 called the ε -insensitive loss function, the loss equals zero if the forecast value is within the
 201 ε -tube and Fig. 6. The second term is used as a measure of the flatness of the function,
 202 Hence, C is referred to as the regularized constant and it determines the trade-off between
 203 the empirical risk and the regularization term. Increasing the value of C will result in an
 204 increasing relative importance of the empirical risk with respect to the regularization term.
 205 ε is called the tube size and it is equivalent to the approximation accuracy placed on the
 206 training data points. Both C and ε are user-prescribed parameters, two positive slack
 207 variables ξ and ξ^* , which represent the distance from actual values to the corresponding
 208 boundary values of ε -tube (Fig. 6), are introduced. Then, Eq. (2) is transformed into the
 209 following constrained form.

$$210 \quad \text{Minimize: } \frac{1}{2} \|\omega\|^2 + C \left(\sum_i^N (\xi_i + \xi_i^*) \right) \quad (4)$$

$$211 \quad \text{Subject to } \begin{cases} \omega_i \phi(x_i) + b_i - d_i \leq \varepsilon + \xi_i^*, i = 1, 2, \dots, N \\ d_i - \omega_i \phi(x_i) - b_i \leq \varepsilon + \xi_i, i = 1, 2, \dots, N \\ \xi_i, \xi_i^*, i = 1, 2, 3, \dots, N \end{cases}$$

212 This constrained optimization problem is solved using the following primal Lagrangian form:

$$213 \quad L = \frac{1}{2} \|\omega\|^2 + C \left(\sum_i^N (\xi_i + \xi_i^*) \right) - \sum_i^N \alpha_i [\omega_i \phi(x_i) + b - d_i + \varepsilon + \xi_i] \\ 214 \quad - \sum_{i=1}^N \alpha_i^* [d_i - \omega_i \phi(x_i) - b + \varepsilon + \xi_i^*] - \sum_i^N (\beta_i \xi_i + \beta_i^* \xi_i^*) \quad (5)$$

215 Eq. (5) is minimized with respect to primal variables ω_i, b, ξ and ξ^* , and maximized with
 216 respect to the nonnegative Lagrangian multipliers $\alpha_i, \alpha_i^*, \beta_i$ and β_i^* , Finally, Karush-Kuhn-
 217 Tucker conditions are applied to the regression, and Eq. (5) has a dual Lagrangian form:

$$218 \quad \nu(\alpha_i, \alpha_i^*) = \sum_{i=1}^N d_i (\alpha_i - \alpha_i^*) - \varepsilon \sum_{i=1}^N (\alpha_i + \alpha_i^*) - \frac{1}{2} \sum_{i=1}^N \sum_{j=1}^N (\alpha_i - \alpha_i^*) (\alpha_j - \alpha_j^*) K(x_i, x_j) \quad (6)$$

219 with the constraints,

$$220 \quad \sum_{i=1}^N (\alpha_i - \alpha_i^*) = 0 \quad \text{And } \alpha_i, \alpha_i^* \in [0, C], i = 1, 2, \dots, N$$

221 In Eq. (6), the Lagrange multipliers satisfy the equality $\alpha_i \alpha_i^* = 0$, The Lagrange multipliers
 222 α_i and α_i^* are calculated, and the optimal desired weight vector of the regression hyperplane is

$$223 \quad \omega^* = \sum_{i=1}^N (\alpha_i - \alpha_i^*) K(x, x_i) \quad (7)$$

224 Therefore, the regression function can be given as

$$225 \quad f(x, \alpha, \alpha^*) = \sum_{i=1}^N (\alpha_i - \alpha_i^*) K(x, x_i) + b \quad (8)$$

226 Here, $K(x, x_i)$ is called the Kernel function. The value of the Kernel is inner product of the two
227 vectors x_i and x_j in the feature space $\phi(x)$ and $\phi(x_j)$, so $K(x, x_j) = \phi(x) \cdot \phi(x_j)$, and function
228 that satisfies Mercer's condition (Vapnik, 1998) can be used as the Kernel Function. In general,
229 three kinds of kernel function are used as follows:

230 Polynomial:

$$231 \quad K(x, x_j) = (x \cdot x_j + 1)^n \quad (9)$$

232 Radial basis function (RBF)

$$233 \quad K(x, x_j) = \exp(-\|x - x_j\|^2 / 2\sigma^2) \quad (10)$$

234 Two-layer neural networks

$$235 \quad K(x, x_j) = \tanh(kx \cdot x_j - \delta)^n \quad (11)$$

236 **3 Study area and data**

237 In this study, Manwan Hydropower in Lancangjiang River is selected as a study site. The
238 monthly flow data from January 1953 to December 2004 are studied. The data set from January
239 1953 to December 1999 is used for calibration whilst that from January 2000 to December 2004 is
240 used for validation (Fig.7). Lancangjiang River is a large river in Asia, which originates from
241 Qinghai-Tibet Plateau, penetrates Yunnan from northwest to the south and passes through Laos,
242 Burma, Thailand, Cambodia and Vietnam, ingresses into South China Sea finally. The river is
243 about 4,500 km long and has a drainage area of 744,000 km². Manwan Hydropower merges on the
244 middle reaches of Lancang River and at borders of Yunxian and Jingdong counties. The catchment
245 area at Manwan dam site is 114,500 km², the length above Manwan is 1,579 km, and the mean
246 elevation is 4,000 km. The average yearly runoff is 1,230 cubic meters per at the dam site. Rainfall
247 provides most of the runoff and snow melt accounts for 10%. Nearly 70% of the annual rainfall
248 occurs from June to September. Locations of Lancang River and Manwan Hydropower are shown
249 in Fig.8 (A).

250 The second study site is at Hongjiadu Hydropower on Wujiang River in southwest China. The
251 monthly flow data from January 1951 to December 2004 are studied. The data set from January
252 1951 to December 1994 is used for calibration whilst that from January 1995 to December 2004 is
253 used for validation (Fig.9). Wujiang River, originating from Wumeng foothill of Yun-Gui Plateau,
254 is the biggest branch at the southern bank of Yangtze River, which covers 87,920km², total length
255 of 1,037km, centralized fall of 2,124m, and with approved installed capacity 8,800MW. Nowadays,
256 Hongjiadu hydropower station is the master regulation reservoir for the cascade hydropower
257 stations on Wujiang River. The catchment area at Hongjiadu dam site is 9,900 km² and the average
258 yearly runoff is 155 cubic meters at the dam site. Rainfall provides most of the runoff. Locations
259 of Wujiang River and Hongjiadu Hydropower are shown in Fig.8 (B).

260
261 In ANN, ANFIS and SVM modeling processes, large attribute values might cause numerical
262 problems because the neurons in ANN and ANFIS are combined Sigmoid function as excitation
263 function, and the kernel values in SVM usually depend on the inner products of feature vectors,
264 such as the linear kernel and the polynomial kernel. There are two main advantages to normalize

265 features before applying ANN, ANFIS and SVM to prediction. One advantage is to avoid
266 attributes in greater numeric ranges dominating those in smaller numeric ranges, and another
267 advantage is to avoid numerical difficulties during the calculation. It is recommended to linearly
268 scale each attribute to the range [-1, +1] or [0, 1]. In the modeling process, the data sets of river
269 flow were scaled to the range between 0 and 1 as follow:

$$270 \quad q'_i = \frac{q_i - q_{\min}}{q_{\max} - q_{\min}} \quad (12)$$

271 where q'_i is the scaled value, q_i is the original flow value and q_{\min} , q_{\max} are respectively
272 the minimum and maximum of flow series.

273 **4. Prediction modeling and input selection**

274 We are interested in hydrological forecasting model that predict outputs from inputs based on
275 past records. There are no fixed rules for developing these AI techniques (ANN, ANFIS, GP,
276 SVM), even though a general framework can be followed based on previous successful
277 applications in engineering (Cheng et al., 2005; Lin et al., 2006; Nayak et al., 2004; Sudheer et al.,
278 2002). The objective of studies focus on predicting discharges using antecedent values is to
279 generalize a relationship of the following form:

$$280 \quad Y = f(X^m) \quad (13)$$

281 where X^m is a m-dimensional input vector consisting of variables $x_1, \dots, x_i, \dots, x_m$, and Y is the output
282 variable. In discharge modeling, values of x_i may be flow values with different time lags and the
283 value Y is generally the flow in the next period. Generally, the number of antecedent values
284 included in the vector X^m is not known a priori.

285 In these AI techniques, being typical in any data-driven prediction models, the selection of
286 appropriate model input vector would play an important role in their successful implementation
287 since it provides the basic information about the system being modeled. The parameters
288 determined as input variables are the numbers of flow values for finding the lags of runoff that
289 have a significant influence on the predicted flow. These influencing values corresponding to
290 different lags can be very well established through a statistical analysis of the data series.
291 Statistical procedures were suggested for identifying an appropriate input vector for a model (Lin
292 et al., 2006; Sudheer et al., 2002). In this study, two statistical methods (i.e. the autocorrelation
293 function (ACF) and the partial autocorrelation function (PACF)) are employed to determine the
294 number of parameters corresponding to different antecedents values. The influencing antecedent
295 discharge patterns can be suggested by the ACF and PACF in the flow at a given time. The ACF
296 and PACF are generally used in diagnosing the order of the autoregressive process and can also be
297 employed in prediction modeling (Lin et al., 2006). The values of ACF and PACF of monthly flow
298 sequence (1953/1~1999/12) is calculated for lag 0 to 24 in Manwan, which are presented in Fig.10.
299 Similarly, the values of ACF and PACF of monthly flow sequence (1951/1~1994/12) is calculated
300 for lag 0 to 24 in Hongjiadu, which are presented in Fig.11. From Fig.10(a) and Fig.11(a), the ACF
301 exhibits the peak at lag 12. In addition, Fig.10(b) and Fig.11(b) showed a significant correlation of
302 PACF at 95% confidence level interval up to 12 months of flow lag. Therefore twelve antecedent
303 flow values have the most information to predict future flow and are considered as input for

304 monthly discharge time series modeling.

305 **5. Model performance evaluation**

306 Some techniques are recommended for hydrological time series forecasting model performance
 307 evaluation according to published literature related to calibration, validation, and application of
 308 hydrological models. Four performance evaluation criteria used in this study are computed as in
 309 the following section.

310 **The coefficient of correlation (R) or its square, the coefficient of determination (R²):** It
 311 describes the degree of collinearity between simulated and measured data, which ranges from -1 to
 312 1, is an index of the degree of linear relationship between observed and simulated data. If R =0, no
 313 linear relationship exists. If R=1 or -1, a perfect positive or negative linear relationship exists. Its
 314 equation is

$$315 \quad R = \frac{\frac{1}{n} \sum_{i=1}^n (Q_0(i) - \bar{Q}_0)(Q_f(i) - \bar{Q}_f)}{\sqrt{\frac{1}{n} \sum_{i=1}^n (Q_0(i) - \bar{Q}_0)^2} * \sqrt{\frac{1}{n} \sum_{i=1}^n (Q_f(i) - \bar{Q}_f)^2}} \quad (14)$$

316 R and R² have been widely used for model evaluation (Lin et al., 2006; Santhi et al., 2001; Van
 317 Liew et al., 2003), though they are oversensitive to high extreme values (outliers) and insensitive
 318 to additive and proportional differences between model predictions and measured data (Legates
 319 and McCabe, 1999).

320 **Nash-Sutcliffe efficiency coefficient (E):** The Nash-Sutcliffe model efficiency coefficient is used
 321 to assess the predictive power of hydrological models (Nash and Sutcliffe, 1970). It is a
 322 normalized statistic that determines the relative magnitude of the residual variance (“noise”)
 323 compared to the measured data variance and indicates how well the plot of observed versus
 324 simulated data fits the 1:1 line (Moriassi et al., 2007). It is defined as:

$$325 \quad E = 1 - \frac{\sum_{i=1}^n (Q_0(i) - Q_f(i))^2}{\sum_{i=1}^n (Q_0(i) - \bar{Q}_0)^2} \quad (15)$$

326 Nash-Sutcliffe efficiencies ranges between (-∞, 1]: E=1 corresponds to a perfect match of
 327 forecasting discharge to the observed data; E=0 shows that the model predictions are as accurate
 328 as the mean of the observed data; and -∞<E<0 occurs when the observed mean is a better predictor
 329 than the model, which indicates unacceptable performance.

330 **Root mean squared error (RMSE):** It is an often used measure of the difference between values
 331 predicted by a model and those actually observed from the thing being modeled. RMSE is one of
 332 the commonly used error index statistics (Lin et al., 2006; Nayak et al., 2004) and is defined as:

$$333 \quad RMSE = \sqrt{\frac{1}{n} \sum_{i=1}^n (Q_f(i) - Q_0(i))^2} \quad (16)$$

334 **Mean absolute percentage error (MAPE):** The MAPE is computed through a term-by-term
 335 comparison of the relative error in the prediction with respect to the actual value of the variable.

336 Thus, the MAPE is an unbiased statistic for measuring the predictive capability of a model. It is a
337 measure of the accuracy in a fitted time series value in statistics and has been used for river flow
338 time series prediction evaluation (Hu et al., 2001). It usually expresses accuracy as a percentage
339 and is defined as:

340

$$341 \quad MAPE = \frac{1}{n} \sum_{i=1}^n \left| \frac{Q_f(i) - Q_0(i)}{Q_0(i)} \right| \times 100 \quad (17)$$

342 where $Q_0(i)$ and $Q_f(i)$ are, respectively, the observed and forecasted discharge and $\overline{Q_0}, \overline{Q_f}$
343 denote their means, and n is the number data points considered.

344 **5. Development of models**

345 ARMA model uses the direct dependence of the previous measurements and depends on the
346 previous innovation of the process in a moving average form. The monthly discharge series, which
347 do fit a normal distribution with respect to the skewness coefficient, can be normalized using a
348 log-transformation function in order to remove the periodicity in the original record (Keskin et al.,
349 2006). In order to choose the appropriate ARMA (p, q) model, the Akaike information criteria
350 (AIC) are used to select the value of p and q, which represent respectively the number of
351 autoregressive orders and the number of moving-average orders of the ARMA model. In this study,
352 the models ARMA (5, 8), (6, 7), (8, 7), (9, 8) and (11, 8), have a relatively minimum AIC value
353 based on flow series in Manwan, and the models ARMA (5, 9), (6, 10), (7, 9), (8, 9) and (10, 11)
354 have a relatively minimum AIC value based on flow series in Hongjiadu. Table 1 and Table 2,
355 respectively, show their AIC values and the performance of alternative ARMA models. Hence,
356 according to their performance indices, ARMA (8, 7) is selected as the ARMA model in Mamwan,
357 and ARMA (6, 10) is selected as the ARMA model in Hongjiadu.

358 In this study, a typical three-layer feed-forward ANN model (Fig. 1) with a back-propagation
359 algorithm is constructed for forecasting monthly discharge time series. The back-propagation
360 training algorithm is a supervised training mechanism and is normally adopted in most of the
361 engineering application. The primary goal is to minimize the error at the output layer by searching
362 for a set of connection strengths that cause the ANN to produce outputs that are equal to or closer
363 to the targets. The neurons of hidden layer use the tan-sigmoid transfer function, and the linear
364 transfer function for output layer. A scaled conjugate gradient algorithm (Moller, 1993) is
365 employed for training, and the training epoch is set to 500. The optimal number of neuron in the
366 hidden layer was identified using a trial and error procedure by varying the number of hidden
367 neurons from 2 to 13. The number of hidden neurons was selected based on the RMSE. The effect
368 of changing the number of hidden neurons on the RMSE of the data set is shown in Fig. 12 and
369 Fig. 13. It can be observed that the effect of the number of neurons assigned to the hidden layer
370 has insignificant effect on the performance of the feed forward model. The numbers of hidden
371 neurons were found to be four and four for Manwan and Hongjiadu, respectively.

372 The ANFIS applies a hybrid learning algorithm that combines the backpropagation gradient
373 descent and the least squares estimate method, which outperforms the original backpropagation
374 algorithm. An essential part of fuzzy logic is fuzzy sets defined by membership functions and rule
375 bases. Shapes of the fuzzy sets are defined by the membership functions. The adjustment of

376 adequate membership function parameters is facilitated by a gradient vector. After determining a
377 gradient vector, the parameters are adjusted and the performance function is minimised via
378 least-squares estimation. For the proposed Sugeno-type model, the overall output is expressed as
379 linear combinations of the resulting parameters. The output f in Fig. 3 can be rewritten as:

$$380 \quad f = \overline{w_1}f_1 + \overline{w_2}f_2 = (\overline{w_1x})p_1 + (\overline{w_1y})q_1 + (\overline{w_1})r_1 + (\overline{w_2x})p_2 + (\overline{w_2y})q_2 + (\overline{w_2})r_2 \quad (18)$$

381 The resulting parameters ($p_1, q_1, r_1, p_2, q_2, r_2$) are computed by the least-squares method.
382 Consequently, the optimal parameters of the ANFIS model can be estimated using the hybrid
383 learning algorithm. For more detail, please refer to Jang and Sun (Jang et al., 1997).

384 GP has the ability to generate the best computer program to describe the relationship between
385 the input and output. In this study, in order to find the optimal monthly flow series forecasting
386 model, the selection of the appropriate parameters of GP evolution is necessary. Although the
387 fine-tuning of algorithm was not the main concern of this paper, we investigated various
388 initialization and run approaches and the adopted GP parameters are presented in Table 3. This
389 setup furnished stable and effective runs throughout experiments. The evolutionary procedures are
390 similar to GAs including defining the fitness function, genetic operators such as crossover,
391 mutation and reproduction and the termination criterion, etc. In GP, the crossover operator is used
392 to swap the subtree from the parents to reproduce the children using mating selection policy rather
393 than exchanging bit strings as in GAs.

394 A kernel function has to be selected from the qualified functions in using SVM. Dibike et al.
395 (2001) applied different kernels in SVR to rainfall- runoff modeling and demonstrated that the
396 radial basis function (RBF) outperforms other kernel functions. Also, many works on the use of
397 SVR in hydrological modeling and forecasting have demonstrated the favorable performance of
398 the RBF (Khan and Coulibaly, 2006; Lin et al., 2006; Liong and Sivapragasam, 2002; Yu et al.,
399 2006). Therefore, the RBF is used as the kernel function for prediction of discharge in this study.
400 There are three parameters in using RBF kernels: C , ε and σ . the accuracy of a SVM model is
401 largely dependent on the selection of the model parameters. However, structured methods for
402 selecting parameters are lacking. Consequently, some kind of model parameter calibration should
403 be made. Recently, there are several methods developed to identify the parameters, such as the
404 simulated annealing algorithms (Pai and Hong, 2005), GA (Pai, 2006) and the shuffled complex
405 evolution algorithm (SCE-UA) (Lin et al., 2006; Yu et al., 2004). The SCE-UA method belongs to
406 the family of evolution algorithm and was presented by Duan et al. (1993). In this study, the
407 SCE-UA is employed as the method of optimizing parameters of SVM and a more comprehensive
408 presentation can be found by Lin et al. (2006). To reach at a suitable choice of these parameters,
409 the RMSE was used to optimize the parameters. Optimal parameters (C, ε, σ) = (19.9373,
410 8.7775e-004, 1.2408) and (C, ε, σ) = (0.5045, 5.0814e-004, 0.6623) were obtained for Manwan
411 and Hongjiadu, respectively.

412 **6. Results and discussion**

413 The Manwan Hydropower, has been studied by Cheng et al. (2005) using ANFIS with
414 discharges of monthly river flow discharges during 1953-2003, and by Lin et al. (2006) using
415 SVM with discharges of monthly river flow discharges during 1974-2003. In their study, the R and
416 RMSE were employed for evaluation model performance. In this paper, in order to identify more

417 suitable models for forecasting future monthly inflows to hydropower reservoirs, the monthly
418 discharge time series data of two study sites in different rivers are applied. For the same basis of
419 comparison, the same training and verification sets, respectively, are used for all the above models
420 developed, whilst the four quantitative standard statistical performance evaluation measures are
421 employed to evaluate the performances of various models developed. Tables 4 and 5 present the
422 results of Manwan and Hongjiadu study sites respectively, in terms of various performance
423 statistics

424 It can be observed from Tables 4 and 5 that various AI methods have good performance during
425 both training and validation, and they outperform ARMA in terms of all the standard statistical
426 measures. For Manwan hydropower, in the training phase, the ANFIS model obtained the best R,
427 RMSE, and E statistics of 0.932, 329.77, and 0.869, respectively; while the SVM model obtained
428 the best MAPE statistics of 12.49. Analyzing the results during testing, it can be observed that the
429 SVM model outperforms all other models. Similarly, for Hongjiadu hydropower, in the training
430 phase, the ANFIS model obtained the best RMSE and E statistics of 887.38 and 0.564,
431 respectively; while the SVM model obtained the best R and MAPE statistics of 0.753 and 28.25,
432 respectively. Analyzing the results during testing, the SVM model obtained the best R and MAPE
433 statistics of 0.823 and 33.77, respectively; while the GP model obtained the best RMSE, and E
434 statistics of 86.07 and 0.654, respectively. RMSE evaluates the residual between observed and
435 forecasted flow, and MAPE measures the mean absolute percentage error of the forecast. R
436 evaluates the linear correlation between the observed and computed flow, while E evaluates the
437 capability of the model in predicting flow values away from the mean. According to the figures in
438 Tables 4 and 5, we can conclude that the best performance of all AI methods developed in this
439 paper is different in terms of the different statistical measures.

440 In addition, in the validation phase as seen in Tables 4 and 5, the values with the ANFIS, GP and
441 SVM model prediction were able to produce a good, near forecast, as compared to those with
442 ARMA and ANN model, whilst it can be concluded that the ANFIS model obtained the best
443 minimum absolute error between the observed and modeled maximum and minimum peak flows
444 in Manwan Hydropower, and the GP and SVM model obtained the best minimum absolute error
445 between the observed and modeled maximum and minimum peak flows, respectively, in
446 Hongjiadu Hydropower. In the validation phase, the SVM model improved the ARMA forecast of
447 about 6.06% and 20.12% reduction in RMSE and MAPE values, respectively; Improvements of
448 the forecast results regarding the R and E were approximately 1.22% and 1.69%, respectively in
449 Manwan Hydropower. In Hongjiadu Hydropower, the GP model obtained the best value of RMSE
450 during the validation phase decreases by 8.77% and the best value of E increases by 11.99%
451 comparing with ARMA; while, the SVM model obtained the best value of R during the validation
452 phase increases by 4.71% and the best value of MAPE decreases by 29.69% comparing with
453 ARMA. Thus the results of this analysis indicate that the ANFIS or SVM is able to obtain the best
454 result in terms of different evaluation measures during the training phase, and the GP or SVM is
455 able to obtain the best result in terms of different evaluation measures during the validation phase.
456 Furthermore, as can be seen from Tables 4 and 5 that the virtues or defect degree of forecasting
457 accuracy is different in terms of different evaluation measures during the training phase and the
458 validation phase. SVM model is able to obtain the better forecasting accuracy in terms of different
459 evaluation measures during the validation phase not only during the training phase but also during
460 the validation phase. The forecasting results of ANFIS model during the validation phase are

461 inferior to the results during the training phase. GP is in the middle or lower level in training
462 phases, but the GP model is able to obtain the better forecasting result in validation phases, and
463 especially the GP model is able to obtain the maximum peak flows among all models developed in
464 Hongjiadu Hydropower. The performances of all prediction models developed in this paper during
465 the training and validation periods in the two study sites are shown in Fig. 14 to 17.

466 **7. Conclusions**

467 An attempt was made in this study to investigate the performance of several AI methods for
468 forecasting monthly discharge time series. The forecasting methods investigated include the ANNs
469 ANFIS techniques, GP models and SVM method. The conventional ARMA is also employed as a
470 benchmarking yardstick for comparison purposes. The monthly discharge data from actual field
471 observed data in the Manwan Hydropower and Hongjiadu Hydropower were employed to develop
472 various models investigated in this study. The methods utilize the statistical properties of the data
473 series with certain amount of lagged input variables. Four standard statistical performance
474 evaluation measures are adopted to evaluate the performances of various models developed.

475 The results obtained in this study indicate that the AI methods are powerful tools to model the
476 discharge time series and can give good prediction performance than traditional time series
477 approaches. The results indicate that the best performance can be obtained by ANFIS, GP and
478 SVM, in terms of different evaluation criteria during the training and validation phases. SVM
479 model is able to obtain the better forecasting accuracy in terms of different evaluation measures
480 during the validation phase during both the training phase and the validation phase. The
481 forecasting results of ANFIS model during the validation phase are inferior to the results during
482 the training phase. GP is in the middle or lower level in training phases, but the GP model is able
483 to obtain the better forecasting result in validation phases. The ANFIS and GP model obtain the
484 maximum peak flows among all models developed in different studies sites, respectively.
485 Therefore, the results of the study are highly encouraging and suggest that ANFIS, GP and SVM
486 approaches are promising in modeling monthly discharge time series, and this may provide
487 valuable reference for researchers and engineers who apply AI methods for modeling long-term
488 hydrological time series forecasting. It is hoped that future research efforts will focus in these
489 directions, i.e. more efficient approach for training multi-layer perceptrons of ANN model, the
490 increased learning ability of the ANFIS model, the fine-tuning of algorithm for selecting more
491 appropriate parameters of GP evolution, saving computing time or more efficient optimization
492 algorithms in searching optimal parameters of SVM model etc to improve the accuracy of the
493 forecast models in terms of different evaluation measures for better planning, design, operation,
494 and management of various engineering systems.

495 **Acknowledgements**

496 This research was supported by the Central Research Grant of Hong Kong Polytechnic University
497 (G-U265), the National Natural Science Foundation of China (No.50679011), Doctor Foundation
498 of higher education institutions of China (No.20050141008).

499 **Reference**

- 500 ASCE Task Committee., 2000a. Artificial neural networks in hydrology-I: Preliminary concepts.
501 *Journal of Hydrologic Engineering*, ASCE 5(2): 115-123.
- 502 ASCE Task Committee., 2000b. Artificial neural networks in hydrology-II: Hydrological
503 applications. *Journal of Hydrologic Engineering*, ASCE5(2): 124-137.
- 504 Asefa, T., Kemblowski, M., McKee, M. and Khalil, A., 2006. Multi-time scale stream flow
505 predictions: The support vector machines approach. *Journal of Hydrology*, 318(1-4): 7-16.
- 506 Bazartseren, B., Hildebrandt, G. and Holz, K.P., 2003. Short-term water level prediction using
507 neural networks and neuro-fuzzy approach. *Neurocomputing*, 55(3-4): 439-450.
- 508 Borrelli, A., De Falco, I., Della Cioppa, A., Nicodemi, M. and Trautteur, G., 2006. Performance of
509 genetic programming to extract the trend in noisy data series. *Physica a-Statistical
510 Mechanics and Its Applications*, 370(1): 104-108.
- 511 Box, G.E.P. and Jenkins, G.M., 1970. *Times series Analysis Forecasting and Control*. Holden-Day,
512 San Francisco.
- 513 Campolo, M., Soldati, A. and Andreussi, P., 2003. Artificial neural network approach to flood
514 forecasting in the River Arno. *Hydrological Sciences Journal*, 48(3): 381-398.
- 515 Chang, L.C. and Chang, F.J., 2001. Intelligent control for modelling of real-time reservoir
516 operation. *Hydrological Processes*, 15(9): 1621-1634.
- 517 Chau, K.W., 2006. Particle swarm optimization training algorithm for ANNs in stage prediction of
518 Shing Mun River. *Journal of Hydrology*, 329(3-4): 363-367.
- 519 Chau, K.W. and Cheng, C.T., 2002. Real-time prediction of water stage with artificial neural
520 network approach. *Lecture Notes in Artificial Intelligence*, 2557: 715.
- 521 Chen, H.L. and Rao, A.R., 2002. Testing hydrologic time series for stationarity. *Journal of
522 Hydrologic Engineering*, 7(2): 129-136.
- 523 Cheng, C.T., Lin, J.Y., Sun, Y.G. and Chau, K.W., 2005. Long-term prediction of discharges in
524 Manwan hydropower using adaptive-network-based fuzzy inference systems models,
525 *Advances in Natural Computation*, Pt 3, Proceedings. *Lecture Notes in Computer Science*.
526 Springer-Verlag Berlin, Berlin, pp. 1152-1161.
- 527 Dibike, Y.B., Velickov, S., Solomatine, D. and Abbott, M.B., 2001. Model induction with support
528 vector machines: Introduction and applications. *Journal of Computing in Civil
529 Engineering*, 15(3): 208-216.
- 530 Dixon, B., 2005. Applicability of neuro-fuzzy techniques in predicting ground-water vulnerability:
531 a GIS-based sensitivity analysis. *Journal of Hydrology*, 309(1-4): 17-38.
- 532 Duan, Q.Y., Gupta, V.K. and Sorooshian, S., 1993. Shuffled complex evolution approach for
533 effective and efficient minimization. *Journal of Optimization Theory and Applications*,
534 76(3): 501-521.
- 535 Haykin, S., 1999. *Neural networks: a comprehensive foundation*. 2nd ed. Upper Saddle River,
536 New Jersey.
- 537 Hu, T.S., Lam, K.C. and Ng, S.T., 2001. River flow time series prediction with a range-dependent
538 neural network. *Hydrological Sciences Journal*, 46(5): 729-745.
- 539 Jang, J.-S.R., 1993. ANFIS: Adaptive-Network-based Fuzzy Inference Systems. *IEEE
540 Transactions on Systems, Man, and Cybernetics*, 23(3): 665-685.
- 541 Jang, J.-S.R., Sun, C.-T. and Mizutani, E., 1997. *Neuro-Fuzzy and Soft Computing: A*

- 542 Computational Approach to Learning and Machine Intelligence. Prentice-Hall, Upper
543 Saddle River, NJ.
- 544 Johari, A., Habibagahi, G. and Ghahramani, A., 2006. Prediction of soil-water characteristic curve
545 using genetic programming. *Journal of Geotechnical and Geoenvironmental Engineering*,
546 132(5): 661-665.
- 547 Keskin, M.E., Taylan, D. and Terzi, O., 2006. Adaptive neural-based fuzzy inference system
548 (ANFIS) approach for modelling hydrological time series. *Hydrological Sciences Journal*,
549 51(4): 588-598.
- 550 Khan, M.S. and Coulibaly, P., 2006. Application of support vector machine in lake water level
551 prediction. *Journal of Hydrologic Engineering*, 11(3): 199-205.
- 552 Koza, J., 1992. *Genetic Programming: On the Programming of Computers by Natural Selection*.
553 MIT Press, Cambridge, MA.
- 554 Legates, D.R. and McCabe, G.J., 1999. Evaluating the use of "goodness-of-fit" measures in
555 hydrologic and hydroclimatic model validation. *Water Resources Research*, 35(1):
556 233-241.
- 557 Lin, J.Y., Cheng, C.T. and Chau, K.W., 2006. Using support vector machines for long-term
558 discharge prediction. *Hydrological Sciences Journal*, 51(4): 599-612.
- 559 Liong, S.Y. et al., 2002. Genetic Programming: A new paradigm in rainfall runoff modeling.
560 *Journal of the American Water Resources Association*, 38(3): 705-718.
- 561 Liong, S.Y. and Sivapragasam, C., 2002. Flood stage forecasting with support vector machines.
562 *Journal of the American Water Resources Association*, 38(1): 173-186.
- 563 Moller, M.F., 1993. A scaled conjugate gradient algorithm for fast supervised learning. *Neural*
564 *Networks*, 6(4): 525-533.
- 565 Moriasi, D.N. et al., 2007. Model evaluation guidelines for systematic quantification of accuracy
566 in watershed simulations. *Transactions of the ASABE*, 50(3): 885-900.
- 567 Muttill, N. and Chau, K.W., 2006. Neural network and genetic programming for modelling coastal
568 algal blooms. *International Journal of Environment and Pollution*, 28(3-4): 223-238.
- 569 Nash, J.E. and Sutcliffe, J.V., 1970. River flow forecasting through conceptual models part I — A
570 discussion of principles. *Journal of Hydrology*, 10(3): 282-290.
- 571 Nayak, P.C., Sudheer, K.P., Rangan, D.M. and Ramasastri, K.S., 2004. A neuro-fuzzy computing
572 technique for modeling hydrological time series. *Journal of Hydrology*, 291(1-2): 52-66.
- 573 Pai, P.-F., 2006. System reliability forecasting by support vector machines with genetic algorithms.
574 *Mathematical and Computer Modelling*, 43(3-4): 262-274.
- 575 Pai, P.-F. and Hong, W.-C., 2005. Support vector machines with simulated annealing algorithms in
576 electricity load forecasting. *Energy Conversion and Management*, 46(17): 2669-2688.
- 577 Salas, J.D., 1993. Analysis and modeling of hydrologic time series. In: Maidment, D.R., Editor,
578 1993. *The McGraw Hill Handbook of Hydrology*, pp. 19.5–19.9.
- 579 Santhi, C. et al., 2001. Validation of the swat model on a large river basin with point and nonpoint
580 sources. *Journal of the American Water Resources Association*, 37(5): 1169-1188.
- 581 Sivapragasam, C., Vincent, P. and Vasudevan, G., 2007. Genetic programming model for forecast
582 of short and noisy data. *Hydrological Processes*, 21(2): 266-272.
- 583 Srikanthan, R. and McMahon, T.A., 2001. Stochastic generation of annual, monthly and daily
584 climate data: A review. *Hydrology and Earth System Sciences*, 5(4): 653-670.
- 585 Sudheer, K.P., Gosain, A.K. and Ramasastri, K.S., 2002. A data-driven algorithm for constructing

- 586 artificial neural network rainfall-runoff models. *Hydrological Processes*, 16(6):
587 1325-1330.
- 588 Van Liew, M.W., Arnold, J.G. and Garbrecht, J.D., 2003. Hydrologic simulation on agricultural
589 watersheds: Choosing between two models. *Transactions of the Asae*, 46(6): 1539-1551.
- 590 Vapnik, V., 1995. *The Nature of Statistical Learning Theory*. Springer, New York.
- 591 Vapnik, V., 1998. *Statistical learning theory*. Wiley, New York.
- 592 Whigam, P.A. and Crapper, P.F., 2001. Modelling Rainfall-Runoff Relationships using Genetic
593 Programming. *Mathematical and Computer Modelling* 33: 707-721.
- 594 Yu, P.S., Chen, S.T. and Chang, I.F., 2006. Support vector regression for real-time flood stage
595 forecasting. *Journal of Hydrology*, 328(3-4): 704-716.
- 596 Yu, X.Y., Liong, S.Y. and Babovic, V., 2004. EC-SVM approach for real-time hydrologic
597 forecasting. *Journal of Hydroinformatics*, 6(3): 209-223.
- 598
- 599

600

601 **Table.1.** AIC value and performance indices of alternative ARMA models for Manwan
602 hydropower

(p, q)	AIC	Training				Validation			
		R	E	RMSE	MAPE	R	E	RMSE	MAPE
(5, 8)	12.043	0.916	0.839	365.60	17.56	0.927	0.878	359.22	15.72
(6, 7)	12.045	0.915	0.838	366.78	17.42	0.925	0.874	355.18	15.56
(8, 7)	11.786	0.922	0.849	354.27	16.77	0.928	0.869	354.35	15.43
(9, 8)	11.813	0.921	0.847	356.98	16.47	0.923	0.856	380.69	15.89
(11, 8)	11.817	0.921	0.848	355.95	16.13	0.928	0.859	376.04	15.26

603

604

605 **Table.2.** AIC value and performance indices of alternative ARMA models for Hongjiadu
606 hydropower

(p, q)	AIC	Training				Validation			
		R	E	RMSE	MAPE	R	E	RMSE	MAPE
(5,9)	9.231	0.722	0.523	91.57	44.06	0.760	0.557	97.32	49.76
(6,10)	9.221	0.725	0.521	91.57	46.42	0.786	0.584	94.34	48.03
(7,9)	9.242	0.724	0.520	91.89	44.91	0.748	0.538	99.39	48.50
(8,9)	9.252	0.726	0.516	92.24	45.56	0.754	0.540	99.21	47.60
(10,11)	9.268	0.722	0.501	93.68	42.30	0.760	0.540	99.22	46.29

607

608

Table 3. Values of primary parameters used in GP runs

Parameter	Value
Terminal set	Variable x, random (0,1)
Function set	+, -, *, /, sin, cos, ^
Population:	2000 individuals
The maximum number of generations:	100
Crossover rate:	0.9
Mutation rate:	0.05
Selection:	Tournament with elitist strategy
Initial population:	Ramped-half-and-half
The maximum depth of tree representation	9

609

610

611 **Table.4.** Forecasting performance indices of models for Manwan hydropower

Model	Training				Validation					
	R	RMSE	MAPE	E	R	RMSE	MAPE	E	Min	Max
Observed									334.0	3821.0
ARMA	0.922	354.27	16.77	0.849	0.928	354.35	15.63	0.869	373.4	3115.7
ANN	0.925	346.31	16.16	0.856	0.932	345.37	14.01	0.867	369.6	3307.8
ANFIS	0.9322	329.77	15.02	0.869	0.9405	335.02	14.30	0.883	343.7	3509.3
GP	0.918	360.96	17.79	0.843	0.9408	334.04	14.69	0.8838	360.1	3321.0
SVM	0.9315	334.07	12.49	0.866	0.9410	332.86	12.49	0.8836	369.0	3333.6

612 Notes: Min means minimum peak flows, and Max means maximum peak flows

613

614

615 **Table.5.** Forecasting performance indices of models for Hongjiadu hydropower

Model	Training				Validation					
	R	RMSE	MAPE	E	R	RMSE	MAPE	E	Min	Max
Observed									25.5	619.0
ARMA	0.727	91.56	46.42	0.521	0.786	94.34	48.03	0.584	11.1	357.0
ANN	0.725	91.16	46.25	0.526	0.786	91.07	46.15	0.612	39.1	358.7
ANFIS	0.751	87.38	47.41	0.564	0.801	88.71	46.67	0.632	17.8	416.9
GP	0.734	90.28	50.29	0.535	0.815	86.07	50.81	0.654	27.6	430.1
SVM	0.753	89.89	28.25	0.539	0.823	87.57	33.77	0.641	24.6	382.8

616 Notes: Min means minimum peak flows, and Max means maximum peak flows

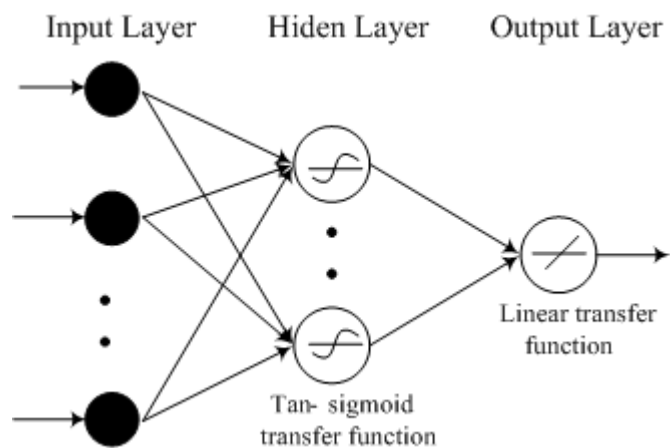
617

618

619

620 List of all figures

621



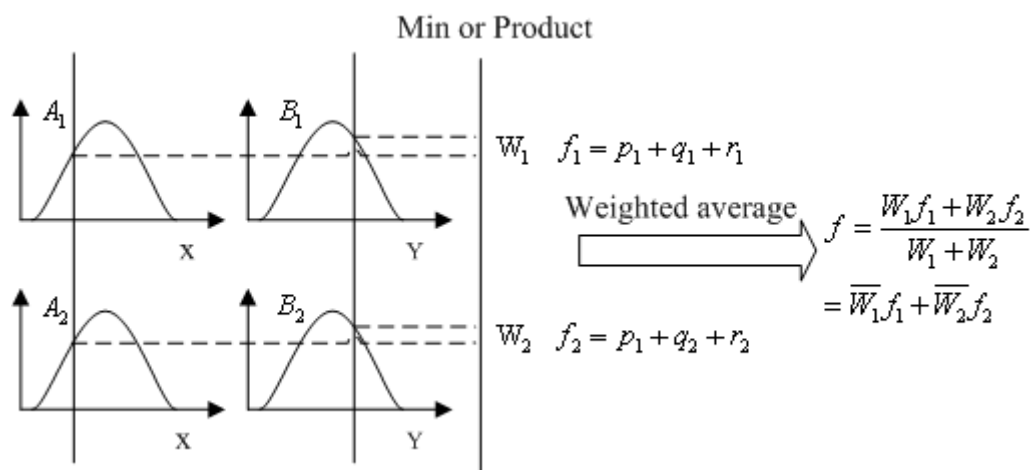
622

623

624

625

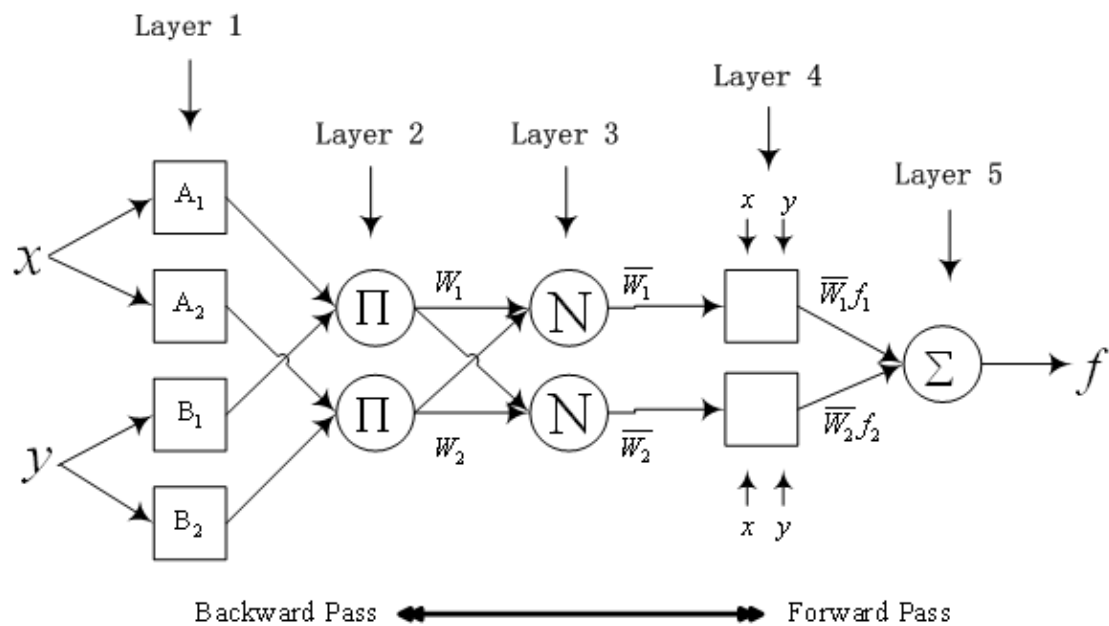
Fig.1. Architecture of three layers feed-forward back-propagation ANN



626

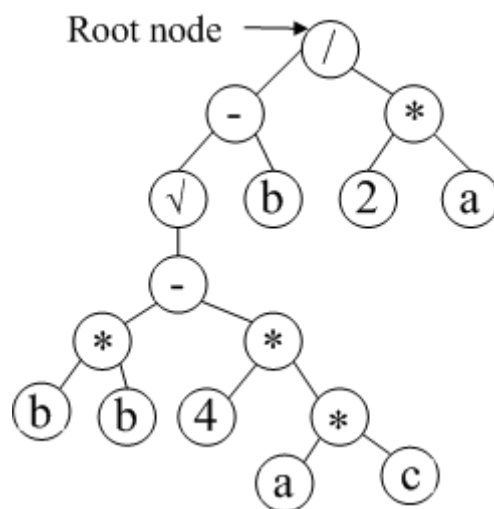
627

Fig.2. Two inputs first-order Sugeno fuzzy model with two rules



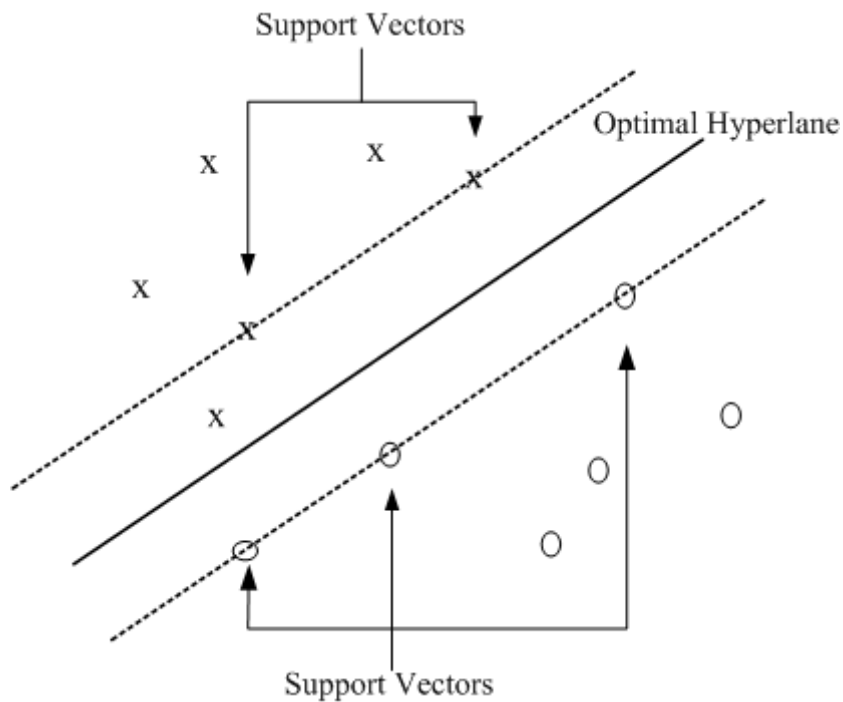
628
629
630
631

Fig.3. Architecture of ANFIS



632
633
634

Fig. 4. GP parse tree representing function $(\sqrt{b^2 - 4ac} - b)/2a$

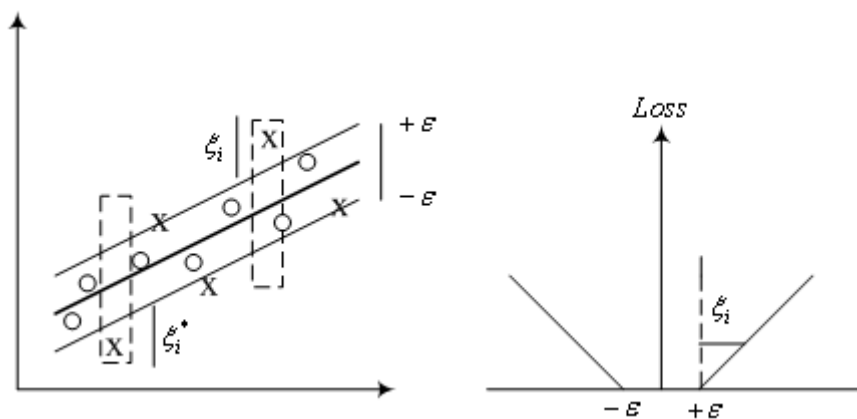


635

636

637

Fig. 5. The basis of the support vector machines.



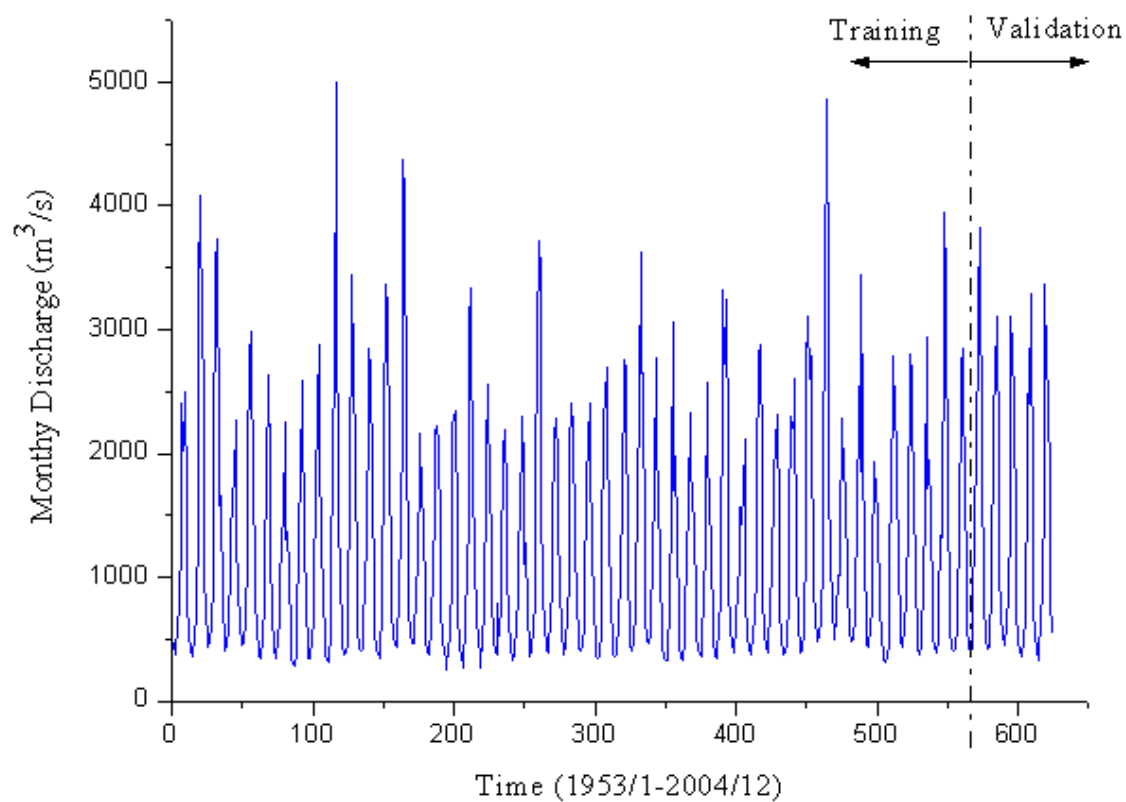
638

639

640

641

Fig.6. The soft margin loss setting for a linear SVM and ϵ -insensitive loss function

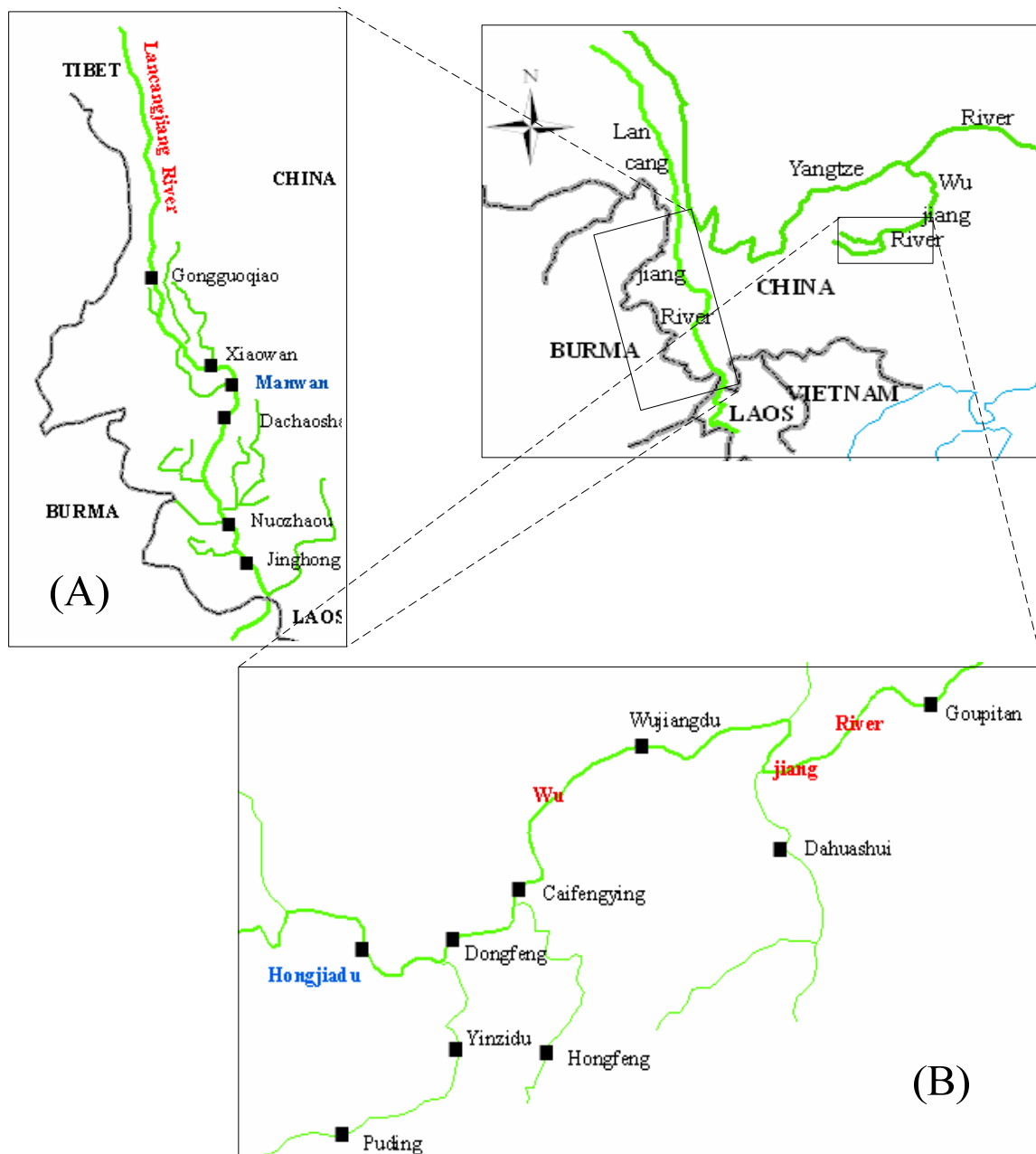


642

643

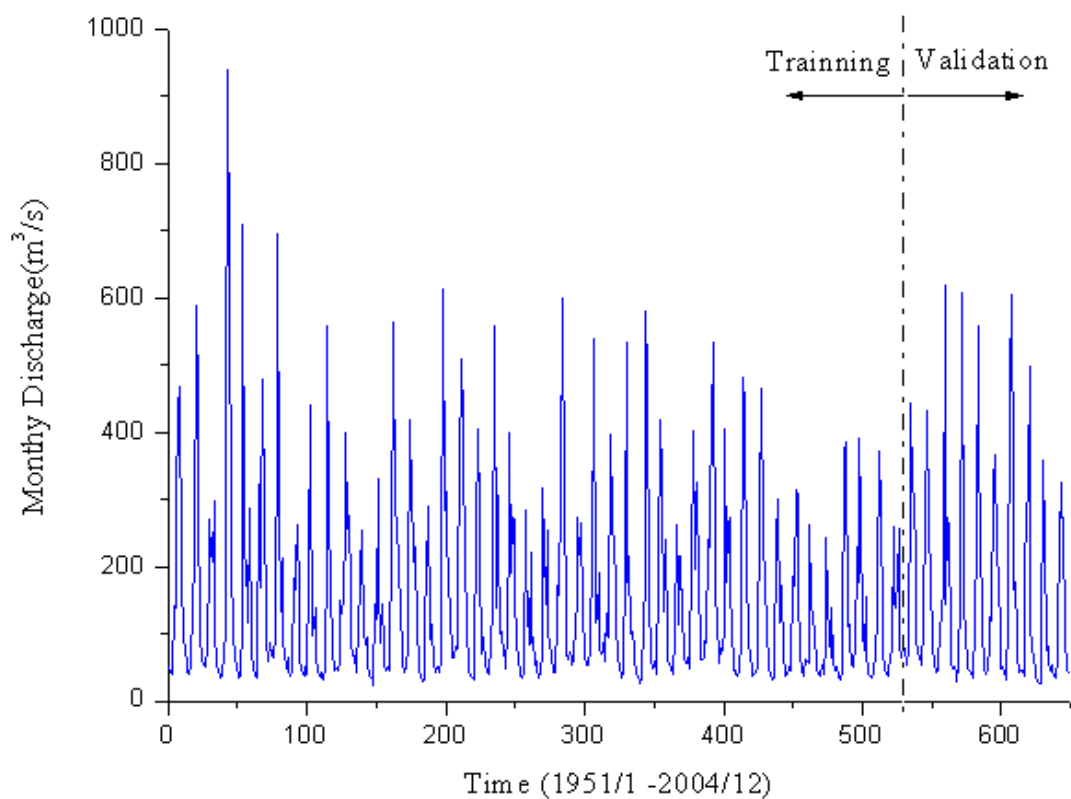
644

Fig. 7. Monthly discharge at Manwan Reservoir



645
 646
 647
 648
 649

Fig. 8 Location of study sites

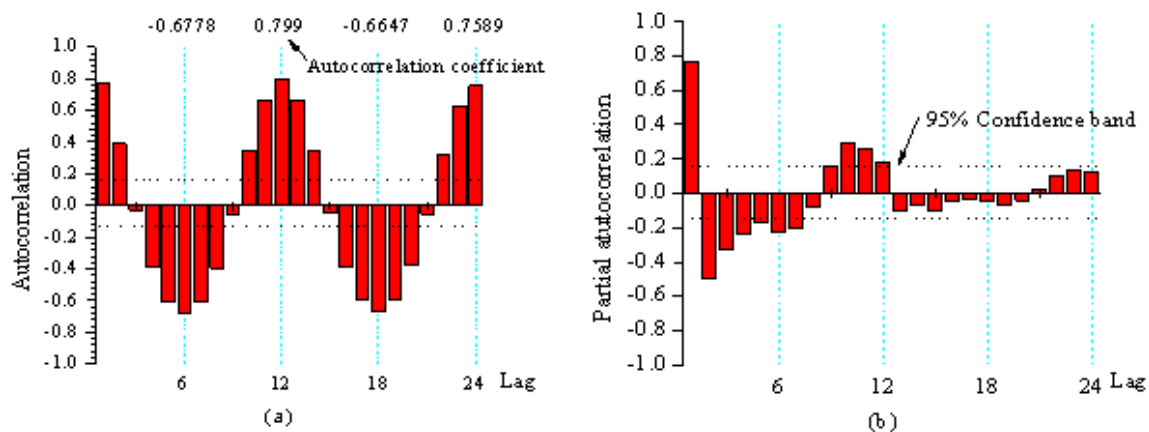


650

651

652

Fig. 9 Monthly discharge at Hongjiadu Reservoir

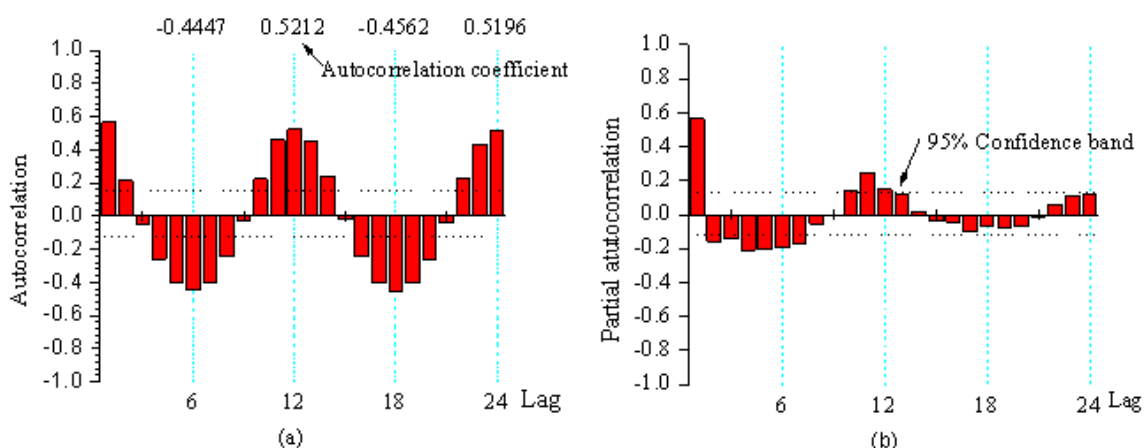


653

654 Fig.10. (a) the autocorrelation function of flow series. (b)The partial autocorrelation function of
655 flow series in Manwan

656

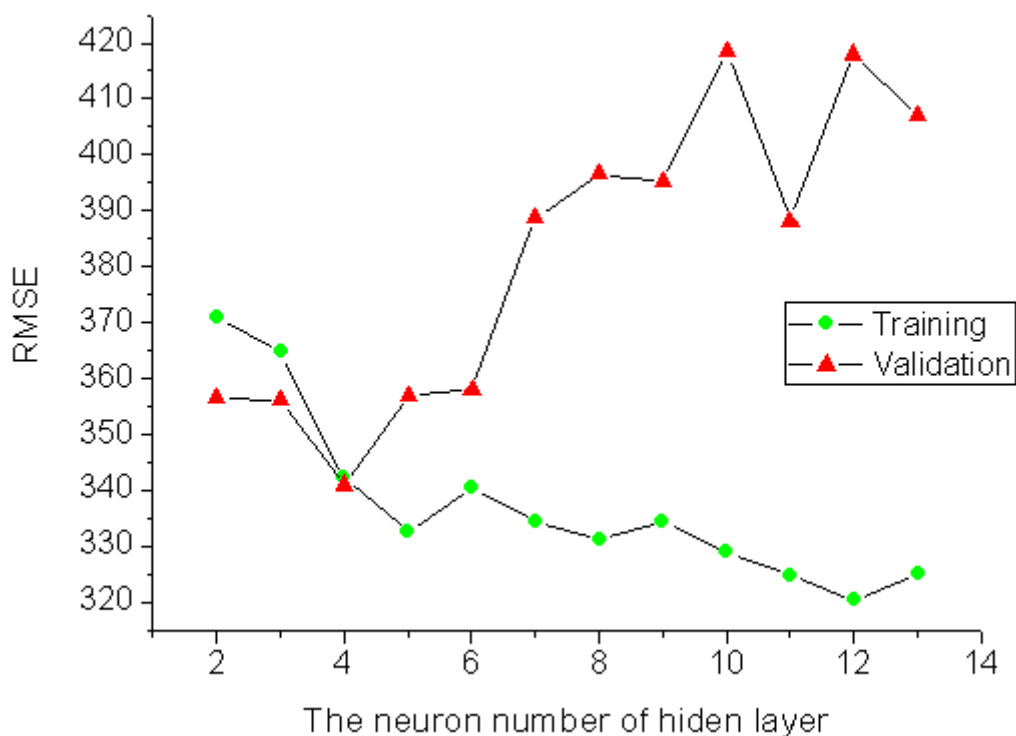
657



658

659 Fig.11 (a) The autocorrelation function of flow series. (b)The partial autocorrelation function of
660 flow series in Hongjiadu.

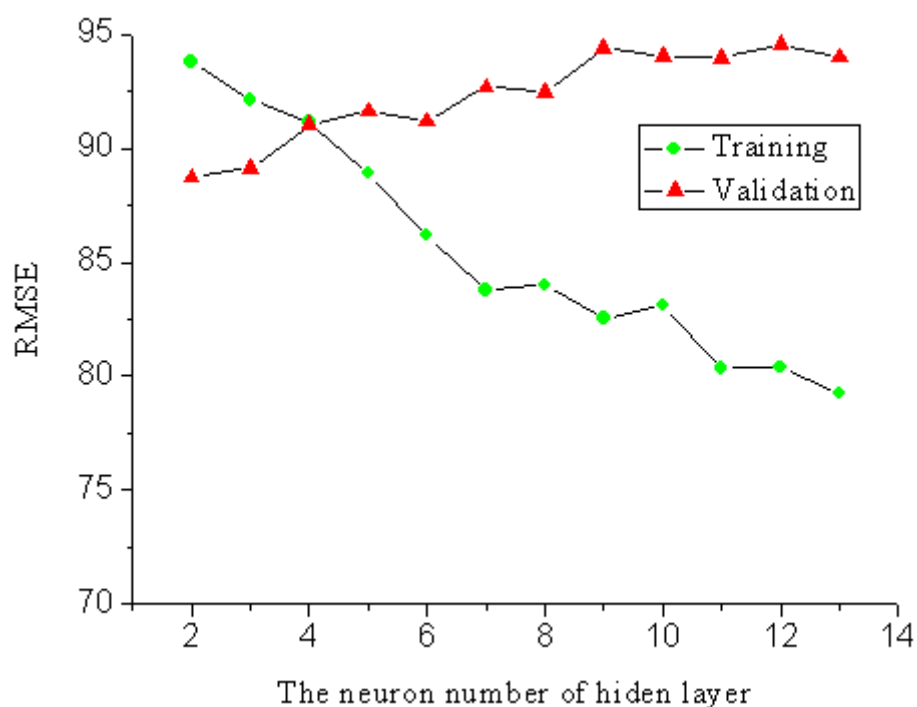
661



662

663 Fig. 12 Sensitivity of the number of nodes in the hidden layer on the RMSE of the neural network
664 for Manwan hydropower

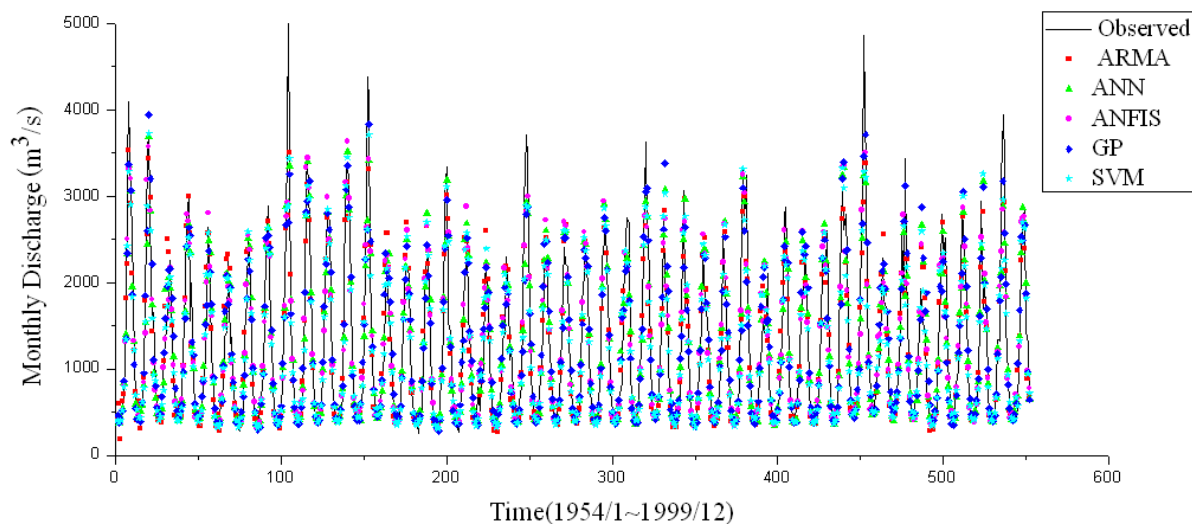
665



666

667 Fig. 13 Sensitivity of the number of nodes in the hidden layer on the RMSE of the neural network
 668 for Hongjiadu hydropower

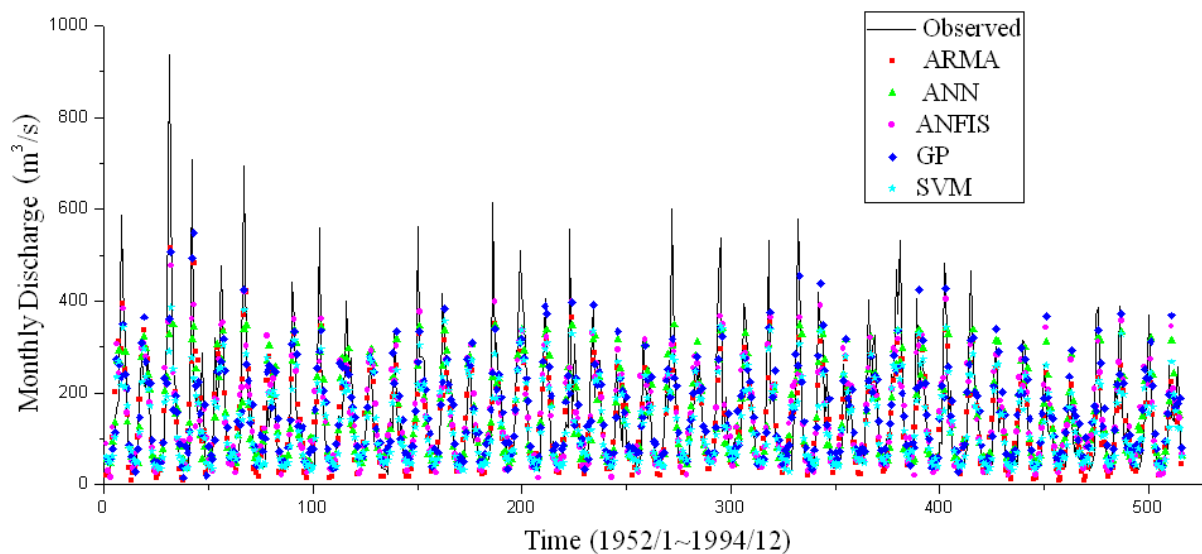
669



670

671 Fig.14 Forecasted and observed flow during training period by ARMA, ANN, ANFIS, GP and
 672 SVM for Manwan hydropower

673

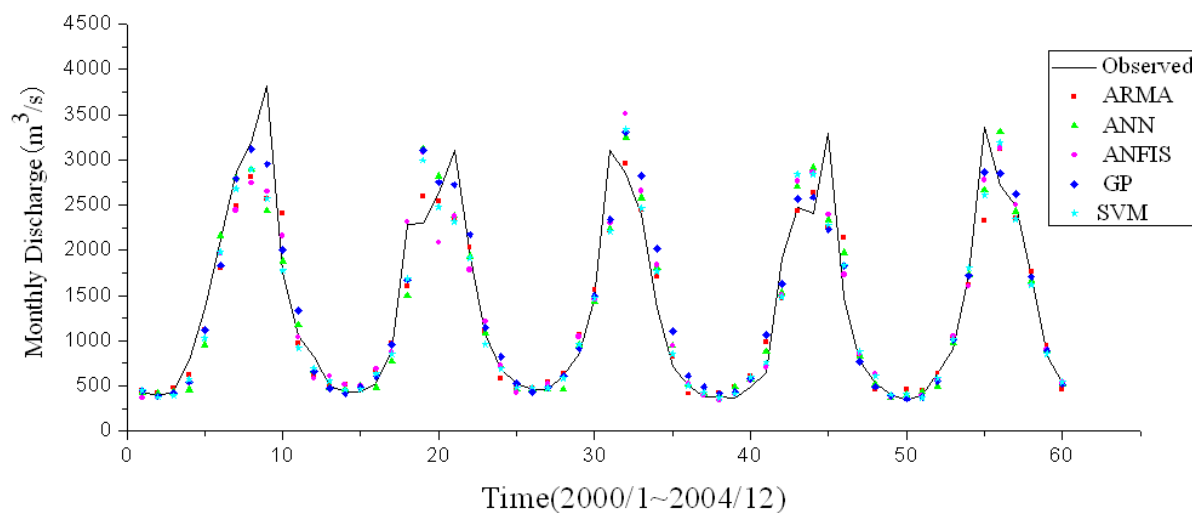


674

675 Fig.15 Forecasted and observed flow during training period by ARMA, ANN, ANFIS, GP and
676 SVM for Hongjiadu hydropower

677

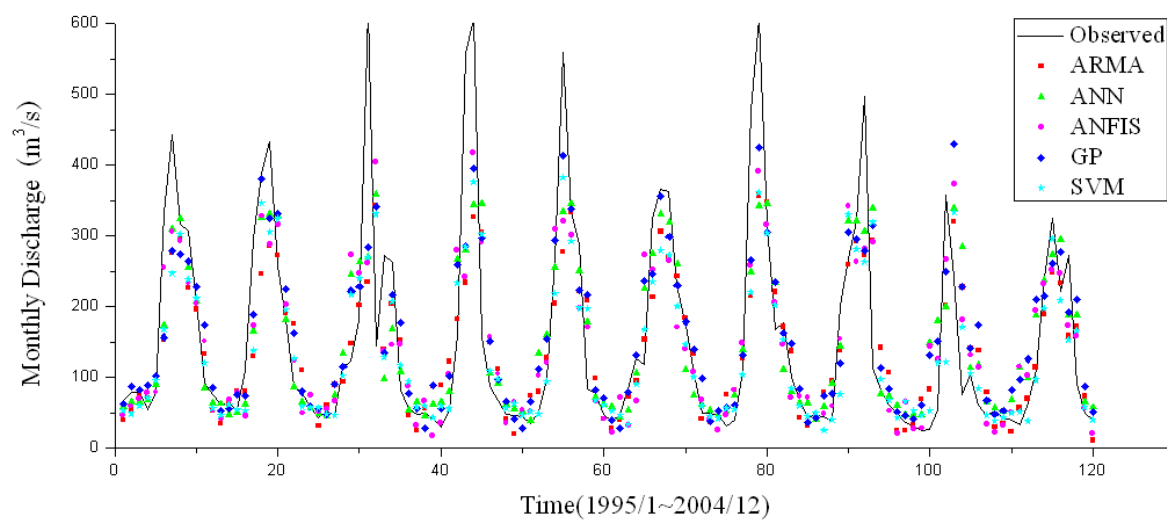
678



679

680 Fig.16 Forecasted and observed flow during validation period by ARMA, ANN, ANFIS, GP and
681 SVM for Manwan hydropower

682



683

684

685

Fig.17 Forecasted and observed flow during validation period by ARMA, ANN, ANFIS, GP and SVM for Hongjiadu hydropower